View Online

Responsive nanogel-based dual fluorescent sensors for temperature and Hg^{2+} ions with enhanced detection sensitivity†

Changhua Li and Shiyong Liu*

Received 9th June 2010, Accepted 4th August 2010
DOI: 10.1039/c0jm01828g

We report on the fabrication of thermoresponsive poly(*N*-isopropylacrylamide) nanogel-based dual fluorescent sensors for temperature and Hg^{2+} ions, and the effects of thermo-induced nanogel collapse on the detection sensitivity of Hg^{2+} ions. Near-monodisperse thermoresponsive nanogels were prepared *via* emulsion polymerization of *N*-isopropylacrylamide (NIPAM) and a novel 1,8-naphthalimide-based polarity-sensitive and Hg^{2+}-reactive fluorescent monomer (NPTUA, ***3***). At room temperature, PNIPAM nanogels labeled with a single type of naphthalimide-based dye (NPTUA) can act as ratiometric Hg^{2+} probes at the nanomolar level. Upon heating above the phase transition temperature, the fluorescence intensity of NPTUA-labeled nanogels in the absence of Hg^{2+} exhibit ~3.4-fold increase due to that NPTUA moieties are now located in a more hydrophobic microenvironment. Moreover, it was observed that the detection sensitivity to Hg^{2+} can be further improved above the nanogel phase transition temperature. At a nanogel concentration of 0.05 g L^{-1} and in the same Hg^{2+} concentration range (0–3.0 equiv.), ~10 fold and ~57 fold increase in fluorescence emission intensity ratio changes can be achieved at 25 and 40 °C, respectively.

Published on 23 November 2010 on http://pubs.rsc.org | doi:10.1039/C0JM01828G
Downloaded by University of Science and Technology of China on 30 November 2010

1. Introduction

In the past decades, the field of probing the presence and concentration of heavy metal ions has received ever-increasing attention owing to emerging environmental and human health issues.[1–3] In particular, as one of the most harmful metal ions, mercury can cause considerable damage to human beings even at low concentrations due to bioaccumulation, long residence, and permanent deterioration in the central nervous and endocrine systems.[4] Thus, the highly sensitive and selective detection and imaging of Hg^{2+} ions in tissues and organisms are quite crucial. In recent years, a variety of fluorescent and colorimetric Hg^{2+} chemosensors have been developed based on small molecules,[5–23] conjugated polymers,[24–26] nanoparticles,[27–35] and biomolecules.[27–30,36–42] Current efforts in this field have focused on the invention of ratiometric,[22,43–47] water-soluble,[25,44,48–51] and cell-permeable Hg^{2+}-sensing ensembles.[15,45,52]

Recently, the concept of fluorescence resonance energy transfer (FRET) has been introduced for designing chemosensors for metal ions to achieve quantitative ratiometric sensing, which can effectively eliminate background interferences and fluctuation of detection conditions through the self-calibration of two emission peaks.[45,47,53–57] Based on the work of Tae and co-workers[58] in 2005, Qian and co-workers[45] reported the first example of a novel small molecule FRET-based ratiometric Hg^{2+} sensor *via* the covalent conjugation of boron dipyrromethene dye (BODIPY) (FRET donor) with leuco-rhodamine derivative (FRET acceptor), taking advantage of the Hg^{2+}-triggered ring-opening reaction of initially nonfluorescent rhodamine in the spirolactam form. However, the rhodamine-based small molecule Hg^{2+} chemosensors are subject to limitations such as poor water solubility and considerable interferences from Ag^{+} and Cu^{2+} ions.[45,59]

Another approach for designing ratiometric metal ion sensors relies on the utilization of intramolecular charge transfer (ICT) processes by employing ICT-based fluorophores whose fluorescence emission band can shift remarkably upon binding or reacting with target metal ions.[46,48,60–62] A typical example is 4-amino-1,8-naphthalimide derivatives. ICT-induced blue shift in the emission peak will occur if the electron-donating capability of amine moieties weakened by replacing with a less electron-rich or electron-deficient substituent.[60,63] Recently, Liu and Tian[46] reported a novel small molecule ratiometric Hg^{2+} sensor based on the 4-amino-1,8-naphthalimide thiourea derivative. The presence of Hg^{2+} ions can induce a remarkable blue shift in the fluorescence emission. Compared to Hg^{2+} chemosensors based on leuco-rhodamine derivatives, 1,8-naphthalimide-based chemosensors possess additional advantages that the interference from Ag^{+} and Cu^{2+} ions can be effectively eliminated. However, the reported 1,8-naphthalimide-based Hg^{2+} chemosensor is barely water-soluble and this limits their practical applications.

It has been well-established that thermoresponsive poly(*N*-isopropylacrylamide) (PNIPAM) nanogels exhibit thermo-induced swelling/collapse behavior in aqueous dispersion, *i.e.*, thermo-induced volume phase transitions (VPTs).[64–67] Therefore, we speculate that the incorporation of ICT-based metal ion-sensing moieties into PNIPAM nanogels should enable the development of highly sensitive and selective chemosensors with combined advantages such as water solubility, biocompatibility, and multifunctional integration. Most importantly, hydrophobic domains within thermo-induced collapsed nanogels can help achieve signal amplification of fluorescent reporter moieties in

CAS Key Laboratory of Soft Matter Chemistry, Department of Polymer Science and Engineering, Hefei National Laboratory for Physical Sciences at the Microscale, University of Science and Technology of China, Hefei, Anhui, 230026, China. E-mail: sliu@ustc.edu.cn

† Electronic supplementary information (ESI) available: Scheme S1 and Fig. S1–S3. See DOI: 10.1039/c0jm01828g

 This journal is © The Royal Society of Chemistry 2010

View Online

Downloaded by University of Science and Technology of China on 30 November 2010
Published on 23 November 2010 on http://pubs.rsc.org | doi:10.1039/C0JM01828G

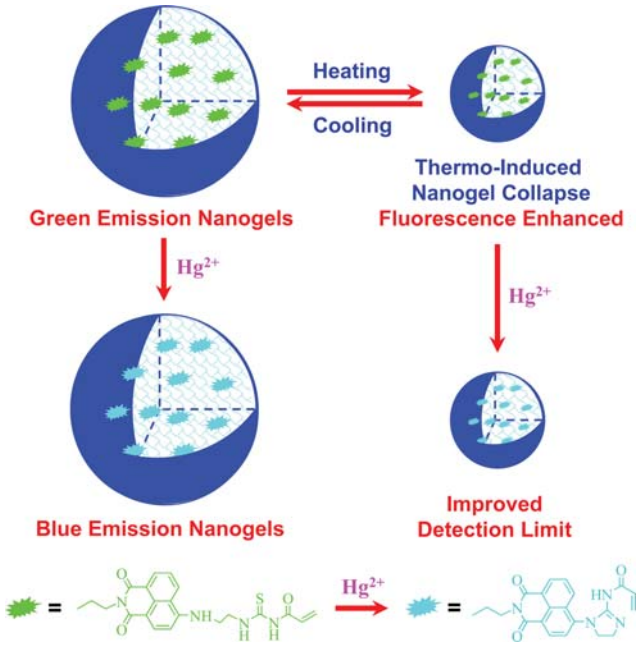

Scheme 1 A schematic illustration of the construction of thermoresponsive PNIPAM nanogel-based dual fluorescent sensors for temperature and Hg^{2+} ions with enhanced detection sensitivity.

sensing ensembles,[59,68–71] which can further enhance the detection sensitivity of metal ions (Scheme 1).

In the current work, we report on the synthesis of thermoresponsive PNIPAM nanogels copolymerized with 1,8-naphthalimide-based polarity-sensitive and Hg^{2+}-reactive monomer (NPTUA, ***3***), which can serve as dual fluorescent sensors for Hg^{2+} ions and temperature (Schemes 1 and S1†). Near-monodisperse thermoresponsive P(NIPAM-*co*-NPTUA) nanogels were prepared *via* emulsion copolymerization of *N*-isopropylacrylamide (NIPAM) and NPTUA (***3***) in the presence of *N*,*N*′-methylenebis(acrylamide) (BIS) and an anionic surfactant. The detection sensitivity and selectivity of as-synthesized nanogels to Hg^{2+} ions at varying temperatures (below and above the nanogel VPT temperatures) have been investigated in detail. We found that NPTUA-labeled PNIPAM nanogels in their swollen state can selectively react with Hg^{2+} over other metal ions, leading to prominent blue shift in fluorescence emission peak. Thus, PNIPAM nanogels labeled with a single type of naphthalimide-based dye can act as ratiometric Hg^{2+} probes at the nanomolar level. Moreover, Hg^{2+} detection sensitivity of NPTUA-labeled PNIPAM nanogels can be considerably enhanced *via* thermo-induced nanogel collapse at elevated temperatures (Scheme 1).

2. Experimental section

Materials

N-Isopropylacrylamide (NIPAM, 97%, Tokyo Kasei Kagyo Co.) was purified by recrystallization from a mixture of benzene and n-hexane (1/3, v/v). Potassium persulfate (KPS) and *N*,*N*′-methylenebis(acrylamide) (BIS) were recrystallized from methanol and ethanol, respectively, and then stored at −20 °C prior to use. Acryloyl chloride (Sinopharm Chemical Reagent Co.) was distilled prior to use. 4-Bromo-1,8-naphthalic anhydride (99% purity), sodium dodecyl sulfate (SDS), n-propylamine, 1,2-ethylenediamine, and all other reagents were purchased from Sinopharm Chemical Reagent Co., Ltd., and used as received. Acetonitrile (MeCN) was dried over CaH_2 and distilled just prior to use. Toluene and 1,4-dioxane were distilled over sodium shavings and benzophenone just prior to use. Nitrate salts (Hg^{2+}, Na^+, K^+, Ag^+, Ca^{2+}, Cu^{2+}, Zn^{2+}, Cd^{2+}, Pb^{2+}, Fe^{2+}, Co^{2+}, Ni^{2+} and Mn^{2+}) were used for all sensing experiments. Water was deionized with a Milli-Q SP reagent water system (Millipore) to a specific resistivity of 18.4 MΩ cm. Acryloyl isothiocyanate was available from our previous work.[59]

Sample synthesis

Synthetic schemes employed for the preparation of 1,8-naphthalimide-based polarity-sensitive and Hg^{2+}-reactive monomer (NPTUA, ***3***), are shown in Scheme S1.†

Preparation of 4-bromo-*N*-n-propyl-1,8-naphthalimide (NP–Br, *1*). A 500 mL round-bottom flask was charged with 4-bromo-1,8-naphthalic anhydride (13.85 g, 50 mmol), n-propylamine (2.96 g, 50 mmol), and 200 mL 1,4-dioxane. The reaction mixture was stirred at reflux for 8 h. After cooling to room temperature, the suspension was poured into 800 mL ice water and then filtrated. After drying in a vacuum oven overnight at room temperature, ***1*** was obtained as a slightly gray solid (14.23 g, yield: 89%). ^{1}H NMR ($CDCl_3$, δ, ppm, TMS, Fig. S1a†): 8.66 (1H, *5*-C*H*), 8.57 (1H, *7*-C*H*), 8.41 (1H, *2*-C*H*), 8.04 (1H, *3*-C*H*), 7.85 (1H, *6*-C*H*), 4.14 (2H, -CH_2CH$_2$CH$_3$), 1.84–1.69 (2H, -CH$_2$CH_2CH$_3$), and 1.07–0.95 (3H, -CH$_2$CH$_2$CH_3).

Preparation of 4-(2-aminoethyl)amino-*N*-n-propyl-1,8-naphthalimide (NP-NH$_2$, *2*). NP-NH_2 was prepared by refluxing ***1*** with an excess of 1,2-ethylenediamine. Into a 100 mL round-bottom flask equipped with a magnetic stirring bar and reflux condenser, ***1*** (3.18 g, 10 mmol) and 1,2-ethylenediamine (50 mL) were charged. The reaction mixture was stirred at reflux for 10 h. After removing all the solvents on a rotary evaporator, the residues were dissolved in THF and precipitated into an excess of water. The crude compound was further purified by recrystallization from toluene. After drying in a vacuum oven overnight at room temperature, NP-NH_2 (***2***) was obtained as an orange crystal (2.32 g, yield: 78%). ^{1}H NMR (d_6-DMSO, δ, ppm, TMS, Fig. S1b†): 8.68 (1H, *5*-C*H*), 8.41 (1H, *7*-C*H*), 8.24 (1H, *2*-C*H*), 7.66 (1H, *6*-C*H*), 6.79 (1H, *3*-C*H*), 3.96 (2H, -CH_2CH$_2$CH$_3$), 2.86 (2H, -CH_2NH$_2$) 1.68–1.54 (2H, -CH$_2$CH_2CH$_3$), and 0.99–0.85 (3H, -CH$_2$CH$_2$CH_3).

Preparation of 1,8-naphthalimide-based monomer (NPTUA, *3*). NP-NH_2 (***2***, 0.59 g, 2.0 mmol) was dissolved in 20 mL of dry MeCN. Freshly prepared acryloyl isothiocyanate (0.23 g, 2.0 mmol) in dry MeCN (10 mL) was then added dropwise over 0.5 h. The reaction mixture was stirred at 40 °C for 3 h. After cooling to room temperature, the precipitates were collected by filtration and washed with dry MeCN for three times. The crude product was further purified by recrystallization from MeCN. After drying in a vacuum oven overnight at room temperature,

View Online

Downloaded by University of Science and Technology of China on 30 November 2010
Published on 23 November 2010 on http://pubs.rsc.org | doi:10.1039/C0JM01828G

NPTUA was obtained as an orange powder (0.55 g, yield: 68%). ^{1}H NMR (d_6-DMSO, δ, ppm, TMS, Fig. S1c†): 8.67 (1H, *5*-C*H*), 8.44 (1H, *7*-C*H*), 8.25 (1H, *2*-C*H*), 7.69 (1H, *6*-C*H*), 6.98 (1H, *3*-C*H*), 6.56 (1H, -C*H* = CHH), 6.36 (1H, -CH = C*H*H), 5.94 (1H, -CH = CH*H*), 3.98 (4H, -CH_2CH$_2$CH$_3$, Ar-NHCH_2-), 3.67 (2H, -CH_2NHC(=S)-) 1.72–1.51 (2H, -CH$_2$CH_2CH$_3$), and 0.96–0.82 (3H, -CH$_2$CH$_2$CH_3).

Synthesis of NPTUA-labeled thermoresponsive P(NIPAM-*co*-NPTUA) nanogels. Typical procedures employed for the preparation of PNIPAM nanogels labeled with NPTUA moieties are as follows. Into a three-neck round-bottom flask equipped with a mechanical Teflon stirrer, a reflux condenser, and a nitrogen-bubbling tube, NIPAM (0.5 g, 4.32 mmol), BIS (15 mg, 97.29 μmol), SDS (4 mg), and deionized water (50 mL) were charged. After degassing by bubbling with N_2 for 30 min and thermostating at 70 °C under mechanical stirring (400 rpm), KPS (25 mg, 92.48 μmol) was introduced to initiate the emulsion polymerization. NPTUA monomer (3 mg, 7.31 μmol) in a mixture of DMSO (0.4 mL) and acetone (5 mL) was then added dropwise over ~4 min. The polymerization was conducted under stirring for 7 h. After cooling to room temperature, the dispersion was passed through glass wool in order to remove particulates and then purified by dialysis (cellulose membrane, molecular weight cut-off: 14 kDa) against deionized water for 5 days. Fresh deionized water was replaced approximately every 4 h.

Characterization

Nuclear magnetic resonance (NMR) spectroscopy. All ^{1}H NMR spectra were recorded on a Bruker AV400 NMR spectrometer (resonance frequency of 400 MHz for ^{1}H) operated in the Fourier transform mode. $CDCl_3$ and d_6-DMSO were used as the solvents.

UV-vis measurements. All UV-Vis spectra were acquired on a Unico UV/Vis 2802PCS spectrophotometer.

Laser light scattering (LLS). A commercial spectrometer (ALV/DLS/SLS-5022F) equipped with a multi-tau digital time correlator (ALV5000) and a cylindrical 22 mW UNIPHASE He–Ne laser (λ_0 = 632 nm) as the light source was employed for dynamic laser light scattering (LLS) measurements. Scattered light was collected at a fixed angle of 90° for duration of ~5 min. Distribution averages and particle size distributions were computed using cumulants analysis and CONTIN routines. All data were averaged over three measurements.

Stopped-flow fluorescence measurements. Stopped-flow fluorescence studies were carried out using a Bio-Logic SFM300/S stopped-flow instrument. The SFM-3/S is a three-syringe (10 mL) instrument in which all step-motor-driven syringes (S1, S2, and S3) can be operated independently to carry out single- or double-mixing. The SFM-300/S stopped-flow device is attached to the MOS-250 spectrometer. Kinetic data were fitted using the program Biokine (Bio-Logic). For the fluorescence emission detection, the excitation and emission wavelengths (10 nm slit widths in both cases) were set at 390 and 482 nm, respectively. The typical dead time is 2.6 ms using the FC-15 flow cell.

Atomic force microscope (AFM). AFM measurements were performed on a Digital Instrument Multimode Nanoscope IIID operating in the tapping mode under ambient conditions. Silicon cantilever (RFESP) with resonance frequency of ~80 kHz and spring constant of ~3 N m^{-1} was used. The set-point amplitude ratio was maintained at 0.7 to minimize sample deformation induced by the tip. The sample was prepared by dip-coating 0.01 g L^{-1} nanogel dispersion onto freshly cleaved mica surface and followed by natural drying.

Fluorescence measurements. Fluorescence spectra were recorded using a RF-5301/PC (Shimadzu) spectrofluorometer. The temperature of the water-jacketed cell holder was controlled by a programmable circulation bath. The slit widths were set at 5 nm for both excitation and emission. For all nanogel-based Hg^{2+} fluorescent sensing experiments, nanogel concentrations are fixed at 0.05 g L^{-1} ([NPTUA] = 5.0 × 10^{-7} M).

3. Results and discussion

Synthesis of P(NIPAM-*co*-NPTUA) nanogels

Synthetic routes employed for the preparation of novel 1,8-naphthalimide-based polarity-sensitive and Hg^{2+}-reactive fluorescent monomer (NPTUA, ***3***) and NPTUA-labeled thermoresponsive nanogels are shown in Scheme S1. The reaction of 4-bromo-1,8-naphthalic anhydride with n-propylamine leads to 4-bromo-*N*-n-propyl-1,8-naphthalimide (NP-*Br*, ***1***) with a yield of 89%. Its chemical structure was confirmed by ^{1}H NMR analysis (Fig. S1†). This was followed by the nucleophilic substitution reaction of NP-*Br* with an excess of 1,2-ethylenediamine. In the final step, the target 1,8-naphthalimide-based monomer (NPTUA, ***3***) was obtained by the reaction of NP-NH_2 with acryloyl isothiocyanate (Scheme S1†). The chemical structures of both NP-NH_2 and NPTUA (***3***) were confirmed by ^{1}H NMR analysis (see Fig. S1†).

P(NIPAM-*co*-NPTUA) nanogels were synthesized *via* free radical emulsion copolymerization of NIPAM and NPTUA in the presence of BIS and SDS at around neutral pH and 70 °C. As-synthesized nanogels with a designed cross-linking density of

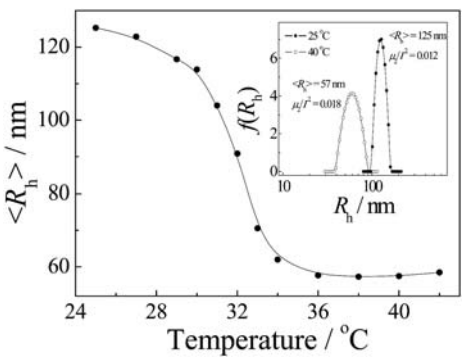

Fig. 1 Temperature-dependence of the intensity average hydrodynamic radius, <R_h>, obtained for 0.05 g L^{-1} aqueous dispersion of P(NIPAM-*co*-NPTUA) nanogels ([NPTUA] = 5.0 × 10^{-7} M). The inset shows typical hydrodynamic radius distributions, $f(R_h)$, of P(NIPAM-*co*-NPTUA) nanogels at 25 and 40 °C, respectively.

 This journal is © The Royal Society of Chemistry 2010

View Online

Downloaded by University of Science and Technology of China on 30 November 2010
Published on 23 November 2010 on http://pubs.rsc.org | doi:10.1039/C0JM01828G

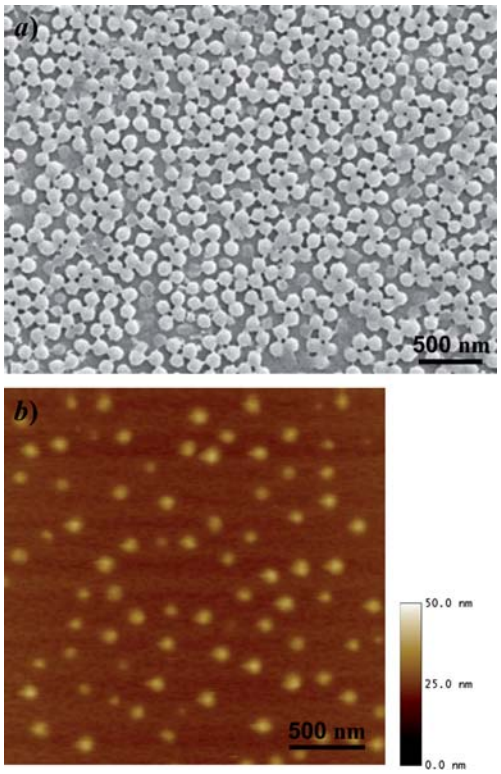

Fig. 2 (a) SEM and (b) AFM height images (Z range is 50 nm) recorded for aqueous dispersion of P(NIPAM-*co*-NPTUA) nanogels at 25 °C.

3.0 wt% were characterized by LLS, SEM, and AFM analysis (Fig. 1 and 2). Aqueous dispersion of P(NIPAM-*co*-NPTUA) nanogels exhibit an intensity-average hydrodynamic radius, $<R_h>$, of 125 nm and a polydispersity index, μ_2/Γ^2, of 0.012 at 25 °C, as revealed by dynamic LLS (Fig. 1). Upon heating to 40 °C, which is above the volume phase transition (VPT) temperature of conventional PNIPAM nanogels, initially swollen nanogels collapse and dynamic LLS reveals an $<R_h>$ of 57 nm and a polydispersity of 0.018. Thus, heating the nanogel dispersion from 25 to 40 °C led to ~10.5 times shrinkage in the hydrodynamic volumes. The molar concentration of NPTUA residues in 10.0 g L^{-1} nanogel dispersion was determined to be $\sim 1.0 \times 10^{-4}$ M based on UV absorbance calibration curve.

SEM and AFM images obtained by drying the aqueous dispersion of P(NIPAM-*co*-NPTUA) nanogels at 25 °C revealed the presence of fairly monodisperse and spherical nanoparticles with average sizes of ~125 and 110 nm, respectively. This agrees reasonably well with that determined by dynamic LLS for collapsed nanogels (Fig. 1). It is well-known that SEM and AFM determine nanoparticle dimensions in the dry state, whereas dynamic LLS report the intensity-average dimensions in the solution.

P(NIPAM-*co*-NPTUA) nanogels as dual sensors for Hg^{2+} ions and temperature

We then investigated the Hg^{2+}-sensing capability of NPTUA-labeled PNIPAM nanogels in their swollen state at 25 °C. It has been well-documented that the modulation of electron-donating capabilities of amine substituent on 1,8-naphthalimide-based

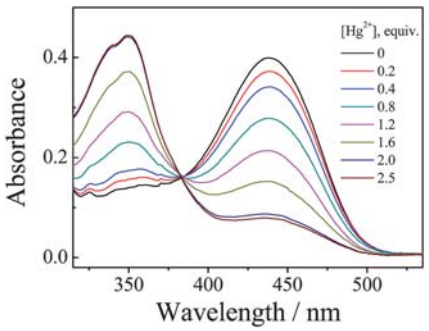

Fig. 3 Absorption spectra recorded for 0.5 g L^{-1} aqueous dispersion of P(NIPAM-*co*- NPTUA) nanogels ([NPTUA] = 5.0×10^{-6} M) upon gradual addition of Hg^{2+} (0–2.5 equiv.) at 25 °C. Each spectrum was acquired 10 min after Hg^{2+} addition.

derivatives can affect both the ICT process and the fluorescence emission bands.[46,48,63] If the amine moieties rendered less electron-rich, ICT-induced blue shifts in the emission maxima can be achieved. In the current work, we designed a novel polymerizable 1,8-naphthalimide-based monomer with the 4-position modified with a substituent that could be selectively uncaged by Hg^{2+} ions, and this process leads to the transformation of secondary amine to tertiary amine residues (Scheme 1). Considering its poor water-solubility, we copolymerized NPTUA monomers into thermoresponsive PNIPAM nanogels to solve this limitation. In the absence of Hg^{2+} ions, P(NIPAM-*co*-NPTUA) nanogels display one major absorption band centered at 438 nm with a corresponding green-colored fluorescence emission maximum at 528 nm (Fig. 3 and 4). The addition of Hg^{2+} ions in aqueous media transforms the thiourea moiety within NPTUA into the imidazoline moiety with considerably weakened electron-donating ability,[46,48] which is accompanied with significant reduction in electron delocalization as compared to that occurred in the NPTUA precursor (Scheme 1). The Hg^{2+}-triggered intramolecular cyclization of thiourea moieties results in ICT-induced blue shifts in fluorescence emissions. Typical absorption and fluorescence emission spectra recorded for the aqueous dispersion of NPTUA-labeled nanogels upon gradual addition of Hg^{2+} ions are shown in Fig. 3 and 4.

As shown in Fig. 3, the UV-vis absorbance intensity of the nanogel dispersion at 438 nm considerably decreases upon gradual addition of Hg^{2+} ions (0–2.5 equiv. relative to that of NPTUA residues), accompanied with the appearance and growth of a new absorption band at ~350 nm. In the Hg^{2+} concentration range investigated, the absorbance intensity exhibits approximately 3.2-fold enhancement at 350 nm and ~5.1-fold decrease at 438 nm. This can be clearly ascribed to Hg^{2+}-induced formation of imidazoline moieties within NPTUA (Scheme 1). Similar processes have been proposed for small molecule naphthalimide-based derivatives possessing comparable chemical structures.[46,48]

The aqueous dispersion of P(NIPAM-*co*-NPTUA) nanogels (0.05 g L^{-1}, [NPTUA] = 5.0×10^{-7} M) in the absence of Hg^{2+} ions exhibit relatively intense fluorescence emission at 528 nm when excited at 390 nm.[46] This indicates that the incorporation of NPTUA moieties into thermoresponsive PNIPAM nanogels does not alter their photophysical properties. As shown in

View Online

Downloaded by University of Science and Technology of China on 30 November 2010
Published on 23 November 2010 on http://pubs.rsc.org | doi:10.1039/C0JM01828G

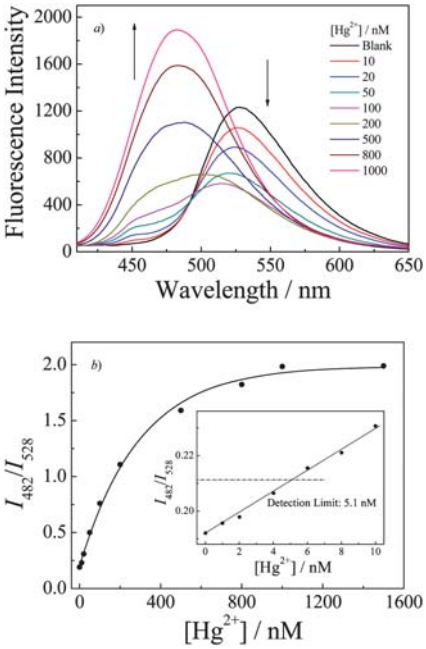

Fig. 4 (a) Fluorescence emission spectra and (b) fluorescence intensity ratio changes (I_{482}/I_{528}; λ_{ex} = 390 nm, slit widths: Ex. 5 nm, Em. 5 nm) recorded for 0.05 g L^{-1} aqueous dispersion of P(NIPAM-*co*-NPTUA) nanogels ([NPTUA] = 5.0 × 10^{-7} M) upon gradual addition of Hg^{2+} (0–3 equiv.) at 25 °C. Each spectrum was acquired 10 min after Hg^{2+} addition. The inset in (b) shows the determination of the detection limit.

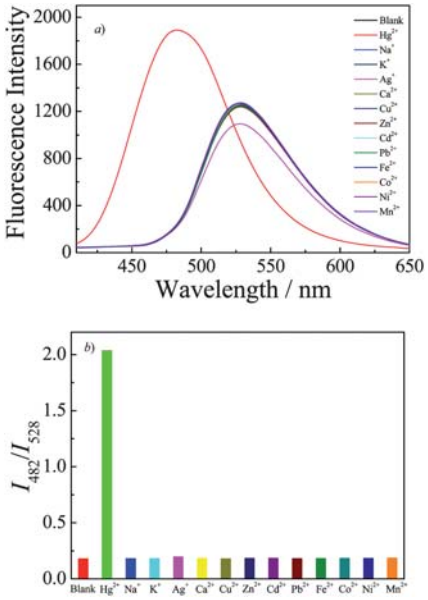

Fig. 5 (a) Fluorescence emission spectra and (b) fluorescence intensity ratio changes (I_{482}/I_{528}; λ_{ex} = 390 nm, slit widths: Ex. 5 nm, Em. 5 nm) recorded for 0.05 g L^{-1} aqueous dispersion of P(NIPAM-*co*-NPTUA) nanogels ([NPTUA] = 5.0 × 10^{-7} M, 25 °C) within 10 min after the addition of 5 equiv. of Hg^{2+}, Na^{+}, K^{+}, Ag^{+}, Ca^{2+}, Cu^{2+}, Zn^{2+}, Cd^{2+}, Pb^{2+}, Fe^{2+}, Co^{2+}, Ni^{2+}, and Mn^{2+}, respectively.

Fig. 4a, upon gradual addition of Hg^{2+} ions, a new fluorescence emission band at 482 nm substantially increases and then stabilizes above ~2.0 equiv. of Hg^{2+} ions (relative to NPTUA residues), which is accompanied with the considerable decrease in fluorescence emission intensity at 528 nm. The dramatic blue shift of fluorescence emission feature is also clearly evident from fluorescence intensity ratio changes, I_{482}/I_{528}, upon Hg^{2+} addition (Fig. 4b). The emission intensity ratios (I_{482}/I_{528}) of imidazoline- to thiourea-derivatized naphthalimide upon excitation at 390 nm vary from 0.20 in the absence of Hg^{2+} to ~1.98 after complete Hg^{2+}-induced conversion to imidazoline-derivatized naphthalimide (in the presence of 3.0 equiv. Hg^{2+} ions), *i.e.*, a *ca.* 10-fold change in emission intensity ratios. If we define the detection limit as the Hg^{2+} concentration at which a 10% change in fluorescence intensity ratio relative to the blank sample can be measured by employing 0.05 g L^{-1} aqueous dispersion of P(NIPAM-*co*-NPTUA) nanogels, the Hg^{2+} detection limit is determined to be ~5.1 nM (Fig. 4b).

The selectivity of P(NIPAM-*co*-NPTUA) nanogels for Hg^{2+} ion sensing was then investigated (Fig. 5 and 6). Among a series of cations including Na^{+}, K^{+}, Ag^{+}, Ca^{2+}, Cu^{2+}, Zn^{2+}, Cd^{2+}, Pb^{2+}, Fe^{2+}, Co^{2+}, Ni^{2+}, Mn^{2+}, and Hg^{2+} (5 equiv.), only Hg^{2+} exhibits the apparent blue shift of UV-vis absorption (yellow to colorless) and fluorescence emission (green to blue transition) within 10 min upon addition. The Hg^{2+}-induced absorption and fluorescence emission changes can also be visualized by the naked eye (Fig. 6). The above results indicate that the incorporation of NPTUA moieties into PNIPAM nanogels does not alter their selective Hg^{2+}-sensing capability. Ag^{+} ions can also induce similar changes in the absorption and fluorescence emission spectra, but it takes ~18 h to complete. This is again in agreement with that reported for small molecule naphthalimide urea derivatives.[46,48] By employing the stopped-flow technique, we further observed that the Hg^{2+}-induced fluorescence "blue shift" process goes to completion within ~6 min (Fig. S2†), which is very fast compared to that of Ag^{+} ions. Thus, we can facilely eliminate the interference of Ag^{+} by employing suitable detection time windows. Based on the above results, we conclude that P(NIPAM-*co*-NPTUA) nanogels possess a high specificity and selectivity for Hg^{2+} ions on a ratiometric basis.

It has been well-established that hydrophobic microenvironments can typically enhance the quantum yields of fluorescent dyes.[67–70] Our recent research interest involves the modulation of emission of caged fluorescent dyes by integrating them into stimuli-responsive polymeric assemblies and nanoparticles to achieve multifunctionality, water-solubility, and biocompatibility, aiming at developing novel drug nanocarriers with imaging and sensing capabilities.[59,72] As P(NIPAM-*co*-NPTUA) nanogels collapse above the phase transition temperature (Fig. 1) accompanied with the formation of more hydrophobic microenvironment, we speculate that the incorporation of NPTUA moieties into thermoresponsive nanogels can act as a novel fluorescent thermometer. We then investigated the temperature-dependent fluorescence emission of NPTUA-labeled nanogel dispersions in the absence of Hg^{2+} ions. As shown in Fig. 7, heating the nanogel dispersion from 25 to 40 °C apparently leads to the increase of emission intensity at 528 nm. Concomitantly, a slight blue shift of the emission maximum from 528 to 511 nm can be observed. This indicated that the quantum yield of NPTUA dyes can be considerably enhanced when the nanogel

 This journal is © The Royal Society of Chemistry 2010

View Online

Downloaded by University of Science and Technology of China on 30 November 2010
Published on 23 November 2010 on http://pubs.rsc.org | doi:10.1039/C0JM01828G

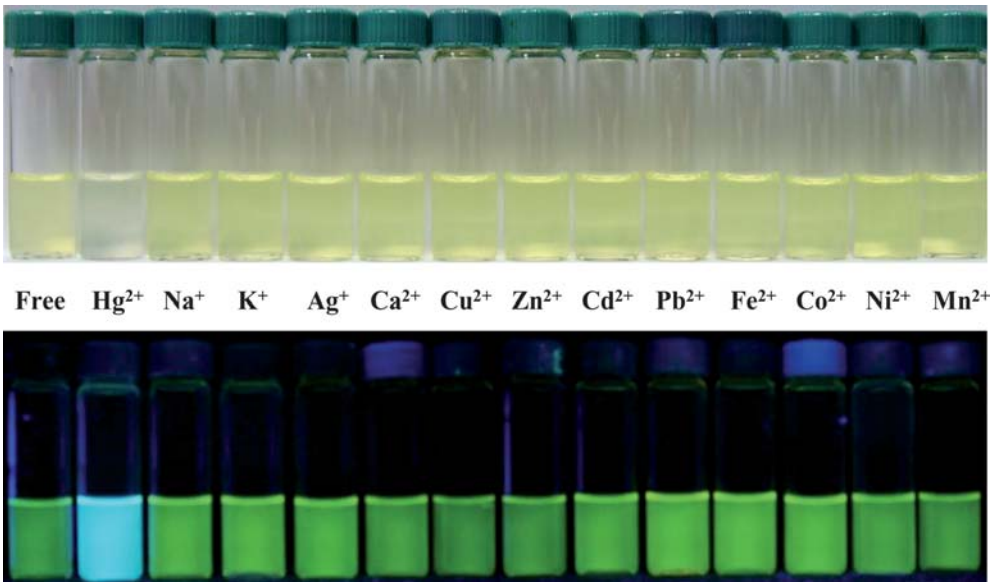

Fig. 6 Optical photographs recorded under visible light (top) and UV lamp (365 nm, bottom) for 1.0 g L^{-1} aqueous dispersion of P(NIPAM-*co*-NPTUA) nanogels ([NPTUA] = 1.0×10^{-5} M) within 10 min after the addition of 5 equiv. of Hg^{2+}, Na^{+}, K^{+}, Ag^{+}, Ca^{2+}, Cu^{2+}, Zn^{2+}, Cd^{2+}, Pb^{2+}, Fe^{2+}, Co^{2+}, Ni^{2+}, and Mn^{2+}, respectively.

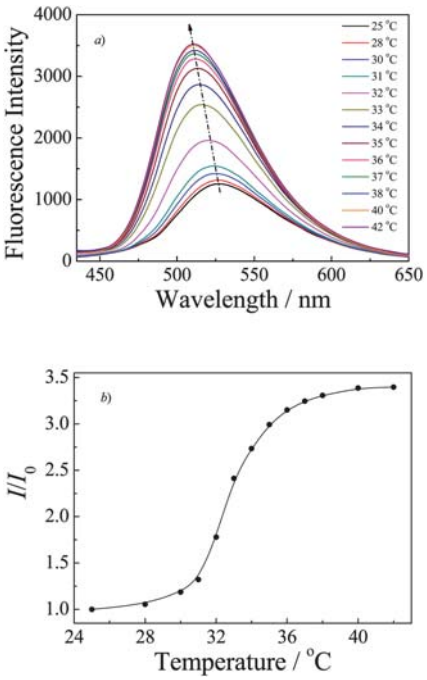

Fig. 7 (a) Fluorescence emission spectra and (b) fluorescence intensity changes (λ_{ex} = 390 nm, λ_{em} = 511 nm; slit widths: Ex. 5 nm, Em. 5 nm) recorded for 0.05 g L^{-1} aqueous dispersion of P(NIPAM-*co*-NPTUA) nanogels ([NPTUA] = 5.0×10^{-7} M) in the temperature range 25–42 °C.

matrix gets more hydrophobic due to thermo-induced collapse. In the narrow temperature range of 30–38 °C, the fluorescence emission intensity at 528 nm exhibits ~2.8 times increase (Fig. 7b). Thus, NPTUA-labeled thermoresponsive nanogels can also act as fluorescent thermometers in the absence of mercury ions.

Effects of thermo-induced nanogel collapse on Hg^{2+}-sensing

Thermo-induced enhancement of fluorescence emission of P(NIPAM-*co*-NPTUA) nanogel dispersions can be further utilized as an approach to achieve signal amplification in Hg^{2+}-sensing experiments. Fig. 8a shows the fluorescence emission

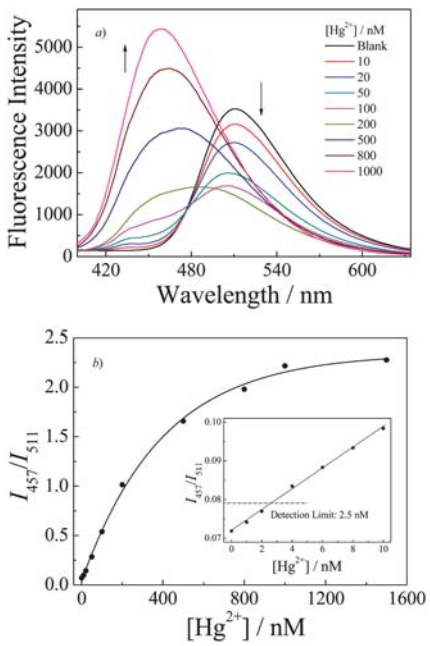

Fig. 8 (a) Fluorescence emission spectra and (b) fluorescence intensity ratio changes (I_{457}/I_{511}; λ_{ex} = 390 nm, slit widths: Ex. 5 nm, Em. 5 nm) recorded at 40 °C for 0.05 g L^{-1} aqueous dispersion of P(NIPAM-*co*-NPTUA) nanogels ([NPTUA] = 5.0×10^{-7} M) upon gradual addition of Hg^{2+} (0–3 equiv.). Each spectrum was acquired 10 min after Hg^{2+} addition. The inset in (b) shows the determination of Hg^{2+} detection limit.

View Online

Downloaded by University of Science and Technology of China on 30 November 2010
Published on 23 November 2010 on http://pubs.rsc.org | doi:10.1039/C0JM01828G

spectra recorded for the aqueous dispersion of P(NIPAM-*co*-NPTUA) nanogels upon gradual addition of Hg^{2+} ions at 40 °C. We can clearly observe the appearance and substantial increase of a new fluorescence emission band at 457 nm upon addition of Hg^{2+} ions, accompanied with the considerable decrease of emission intensity at 511 nm. The new emission band at ~457 nm tends to stabilize out in the presence of >2.0 equiv. of Hg^{2+} ions (relative to NPTUA residues). Fig. 8b plots the Hg^{2+} concentration-dependence of fluorescence intensity ratio changes, I_{457}/I_{511}, which is again ascribed to Hg^{2+}-induced transformation of naphthalimide-thiourea to naphthalimide-imidazoline derivatives. We can tell from Fig. 8b that the emission intensity ratios, I_{457}/I_{511}, increase from 0.04 for the blank sample to 2.29 in the presence of 3.0 equiv. of Hg^{2+} ions.

In the same Hg^{2+} concentration range (0–3.0 equiv.) for 0.05 g L^{-1} P(NIPAM-*co*-NPTUA) nanogel dispersion, ~10 fold and ~57 fold increase in fluorescence emission intensity ratio changes can be achieved at 25 and 40 °C, respectively. This means that Hg^{2+} detection above the VPT temperature of P(NIPAM-*co*-NPTUA) nanogels will be more sensitive, as compared to that below the VPT temperatures. We thus established thermo-induced collapse of thermoresponsive PNIPAM nanogels can be successfully utilized to achieve signal amplification and much better detection sensitivity.

From Fig. 8b, we can also read out a Hg^{2+} detection limit of 2.5 nM for 0.05 g L^{-1} P(NIPAM-*co*-NPTUA) nanogel dispersions at 40 °C, which is again much better than that at 25 °C (5.1 nM). Fig. S3† plots the Hg^{2+} ion concentration dependence of normalized fluorescence intensities of emission band ascribed to the naphthalimide-imidazoline derivative at 25 °C (λ_{em} = 482 nm) and 40 °C (λ_{em} = 457 nm), respectively. In both cases, we can clearly observe the almost linear increase of emission intensities with increasing Hg^{2+} concentrations. Similarly, if we define the detection limit as the Hg^{2+} concentration at which a 10% emission enhancement can be measured by employing 0.05 g L^{-1} aqueous dispersion of the P(NIPAM-*co*-NPTUA) nanogels, the Hg^{2+} detection limits again considerably improve from ~13.3 nM to ~4.1 nM upon the increase in temperature from 25 to 40 °C (Fig. S3†).

4. Conclusions

In summary, we reported the fabrication of thermoresponsive PNIPAM nanogel-based dual fluorescent sensors for temperature and Hg^{2+} ions, and investigated the effects of thermo-induced nanogel collapse on the detection sensitivity. A novel 1,8-naphthalimide-based polarity-sensitive and Hg^{2+}-reactive fluorescent monomer (NPTUA) was synthesized. Near-monodisperse thermoresponsive NPTUA-labeled PNIPAM nanogels were prepared *via* the free radical emulsion copolymerization technique. The nanogel-based chemosensors possess a high selectivity and sensitivity for Hg^{2+} at room temperature, achieving a detection limit at the nanomolar level on a ratiometric basis. Thermo-induced collapse of P(NIPAM-*co*-NPTUA) nanogel have been successfully utilized to further enhance the detection sensitivity. In the same Hg^{2+} concentration range (0–3.0 equiv.) for 0.05 g L^{-1} nanogel dispersion, ~10 fold and ~57 fold increase in fluorescence emission intensity ratio changes can be achieved at 25 and 40 °C, respectively. To the best of our knowledge, this work represents the first report of successful integration of stimuli-responsive nanogels with well-developed small molecule reaction-based selective metal ion sensing moieties.

Acknowledgements

The financial support of National Natural Scientific Foundation of China (NNSFC) Project (20874092) and Specialized Research Fund for the Doctoral Program of Higher Education (SRFDP) are gratefully acknowledged.

References

1 M. Beija, C. A. M. Afonso and J. M. G. Martinho, *Chem. Soc. Rev.*, 2009, **38**, 2410–2433.
2 J. S. Kim and D. T. Quang, *Chem. Rev.*, 2007, **107**, 3780–3799.
3 L. Basabe-Desmonts, D. N. Reinhoudt and M. Crego-Calama, *Chem. Soc. Rev.*, 2007, **36**, 993–1017.
4 T. W. Clarkson, L. Magos and G. J. Myers, *N. Engl. J. Med.*, 2003, **349**, 1731–1737.
5 D. G. Cho and J. L. Sessler, *Chem. Soc. Rev.*, 2009, **38**, 1647–1662.
6 E. M. Nolan and S. J. Lippard, *Chem. Rev.*, 2008, **108**, 3443–3480.
7 H. N. Kim, M. H. Lee, H. J. Kim, J. S. Kim and J. Yoon, *Chem. Soc. Rev.*, 2008, **37**, 1465–1472.
8 E. M. Nolan and S. J. Lippard, *J. Am. Chem. Soc.*, 2007, **129**, 5910–5918.
9 C. S. Lim, D. W. Kang, Y. S. Tian, J. H. Han, H. L. Hwang and B. R. Cho, *Chem. Commun.*, 2010, **46**, 2388–2390.
10 D. Wu, A. B. Descalzo, F. Weik, F. Emmerling, Z. Shen, X. Z. You and K. Rurack, *Angew. Chem., Int. Ed.*, 2008, **47**, 193–197.
11 S. V. Wegner, A. Okesli, P. Chen and C. A. He, *J. Am. Chem. Soc.*, 2007, **129**, 3474–3475.
12 J. V. Ros-Lis, M. D. Marcos, R. Martinez-Manez, K. Rurack and J. Soto, *Angew. Chem., Int. Ed.*, 2005, **44**, 4405–4407.
13 A. Ono and H. Togashi, *Angew. Chem., Int. Ed.*, 2004, **43**, 4300–4302.
14 E. M. Nolan and S. J. Lippard, *J. Am. Chem. Soc.*, 2003, **125**, 14270–14271.
15 W. Y. Lin, X. W. Cao, Y. D. Ding, L. Yuan and L. L. Long, *Chem. Commun.*, 2010, **46**, 3529–3531.
16 X. F. Guo, X. H. Qian and L. H. Jia, *J. Am. Chem. Soc.*, 2004, **126**, 2272–2273.
17 J. J. Du, J. L. Fan, X. J. Peng, P. P. Sun, J. Y. Wang, H. L. Li and S. G. Sun, *Org. Lett.*, 2010, **12**, 476–479.
18 A. B. Descalzo, R. Martinez-Manez, R. Radeglia, K. Rurack and J. Soto, *J. Am. Chem. Soc.*, 2003, **125**, 3418–3419.
19 A. Coskun and E. U. Akkaya, *J. Am. Chem. Soc.*, 2006, **128**, 14474–14475.
20 E. Coronado, J. R. Galan-Mascaros, C. Marti-Gastaldo, E. Palomares, J. R. Durrant, R. Vilar, M. Gratzel and M. K. Nazeeruddin, *J. Am. Chem. Soc.*, 2005, **127**, 12351–12356.
21 M. G. Choi, Y. H. Kim, J. E. Namgoong and S. K. Chang, *Chem. Commun.*, 2009, 3560–3562.
22 X. H. Cheng, Q. Q. Li, J. G. Qin and Z. Li, *ACS Appl. Mater. Interfaces*, 2010, **2**, 1066–1072.
23 A. Caballero, R. Martinez, V. Lloveras, I. Ratera, J. Vidal-Gancedo, K. Wurst, A. Tarraga, P. Molina and J. Veciana, *J. Am. Chem. Soc.*, 2005, **127**, 15666–15667.
24 S. W. Thomas, G. D. Joly and T. M. Swager, *Chem. Rev.*, 2007, **107**, 1339–1386.
25 C. J. Qin, X. F. Wu, B. X. Gao, H. Tong and L. X. Wang, *Macromolecules*, 2009, **42**, 5427–5429.
26 X. F. Liu, Y. L. Tang, L. H. Wang, J. Zhang, S. P. Song, C. H. Fan and S. Wang, *Adv. Mater.*, 2007, **19**, 1471–1474.
27 J. S. Lee, M. S. Han and C. A. Mirkin, *Angew. Chem., Int. Ed.*, 2007, **46**, 4093–4096.
28 W. W. Guo, J. P. Yuan and E. K. Wang, *Chem. Commun.*, 2009, 3395–3397.
29 R. Freeman, T. Finder and I. Willner, *Angew. Chem., Int. Ed.*, 2009, **48**, 7818–7821.
30 J. S. Lee and C. A. Mirkin, *Anal. Chem.*, 2008, **80**, 6805–6808.

 This journal is © The Royal Society of Chemistry 2010

View Online

31 M. Rex, F. E. Hernandez and A. D. Campiglia, *Anal. Chem.*, 2006, **78**, 445–451.
32 S. J. Lee, J. E. Lee, J. Seo, I. Y. Jeong, S. S. Lee and J. H. Jung, *Adv. Funct. Mater.*, 2007, **17**, 3441–3446.
33 C. C. Huang, Z. Yang, K. H. Lee and H. T. Chang, *Angew. Chem., Int. Ed.*, 2007, **46**, 6824–6828.
34 C. C. Huang and H. T. Chang, *Anal. Chem.*, 2006, **78**, 8332–8338.
35 G. K. Darbha, A. Ray and P. C. Ray, *ACS Nano*, 2007, **1**, 208–214.
36 C. W. Liu, C. C. Huang and H. T. Chang, *Anal. Chem.*, 2009, **81**, 2383–2387.
37 X. J. Zhu, S. T. Fu, W. K. Wong, H. P. Guo and W. Y. Wong, *Angew. Chem., Int. Ed.*, 2006, **45**, 3150–3154.
38 L. B. Zhang, L. Tao, B. L. Li, L. Jing and E. K. Wang, *Chem. Commun.*, 2010, **46**, 1476–1478.
39 S. J. Ou, Z. H. Lin, C. Y. Duan, H. T. Zhang and Z. P. Bai, *Chem. Commun.*, 2006, 4392–4394.
40 Y. Miyake, H. Togashi, M. Tashiro, H. Yamaguchi, S. Oda, M. Kudo, Y. Tanaka, Y. Kondo, R. Sawa, T. Fujimoto, T. Machinami and A. Ono, *J. Am. Chem. Soc.*, 2006, **128**, 2172–2173.
41 M. Matsushita, M. M. Meijler, P. Wirsching, R. A. Lerner and K. D. Janda, *Org. Lett.*, 2005, **7**, 4943–4946.
42 I. B. Kim and U. H. F. Bunz, *J. Am. Chem. Soc.*, 2006, **128**, 2818–2819.
43 C. Y. Li, X. B. Zhang, L. Qiao, Y. Zhao, C. M. He, S. Y. Huan, L. M. Lu, L. X. Jian, G. L. Shen and R. Q. Yu, *Anal. Chem.*, 2009, **81**, 9993–10001.
44 M. Q. Tian and H. Ihmels, *Chem. Commun.*, 2009, 3175–3177.
45 X. L. Zhang, Y. Xiao and X. H. Qian, *Angew. Chem., Int. Ed.*, 2008, **47**, 8025–8029.
46 B. Liu and H. Tian, *Chem. Commun.*, 2005, 3156–3158.
47 A. Ben Othman, J. W. Lee, J. S. Wu, J. S. Kim, R. Abidi, P. Thuery, J. M. Strub, A. Van Dorsselaer and J. Vicens, *J. Org. Chem.*, 2007, **72**, 7634–7640.
48 B. Leng, L. Zou, J. B. Jiang and H. Tian, *Sens. Actuators, B*, 2009, **140**, 162–169.
49 J. V. Ros-Lis, R. Martinez-Manez, K. Rurack, F. Sancenon, J. Soto and M. Spieles, *Inorg. Chem.*, 2004, **43**, 5183–5185.
50 E. M. Nolan, M. E. Racine and S. J. Lippard, *Inorg. Chem.*, 2006, **45**, 2742–2749.
51 T. J. Dickerson, N. N. Reed, J. J. LaClair and K. D. Janda, *J. Am. Chem. Soc.*, 2004, **126**, 16582–16586.
52 S. Yoon, E. W. Miller, Q. He, P. H. Do and C. J. Chang, *Angew. Chem., Int. Ed.*, 2007, **46**, 6658–6661.
53 Z. X. Han, X. B. Zhang, L. Zhuo, Y. J. Gong, X. Y. Wu, J. Zhen, C. M. He, L. X. Jian, Z. Jing, G. L. Shen and R. Q. Yu, *Anal. Chem.*, 2010, **82**, 3108–3113.
54 E. M. W. M. Van Dongen, L. M. Dekkers, K. Spijker, E. W. Meijer, L. W. J. Klomp and M. Merkx, *J. Am. Chem. Soc.*, 2006, **128**, 10754–10762.
55 W. Qiao, M. Mooney, A. J. Bird, D. R. Winge and D. J. Eide, *Proc. Natl. Acad. Sci. U. S. A.*, 2006, **103**, 8674–8679.
56 V. S. Jisha, A. J. Thomas and D. Ramaiah, *J. Org. Chem.*, 2009, **74**, 6667–6673.
57 Z. G. Zhou, M. X. Yu, H. Yang, K. W. Huang, F. Y. Li, T. Yi and C. H. Huang, *Chem. Commun.*, 2008, 3387–3389.
58 Y. K. Yang, K. J. Yook and J. Tae, *J. Am. Chem. Soc.*, 2005, **127**, 16760–16761.
59 J. M. Hu, C. H. Li and S. Y. Liu, *Langmuir*, 2010, **26**, 724–729.
60 Z. C. Xu, Y. Xiao, X. H. Qian, J. N. Cui and D. W. Cui, *Org. Lett.*, 2005, **7**, 889–892.
61 X. J. Peng, J. J. Du, J. L. Fan, J. Y. Wang, Y. K. Wu, J. Z. Zhao, S. G. Sun and T. Xu, *J. Am. Chem. Soc.*, 2007, **129**, 1500.
62 Y. Shiraishi, S. Sumiya and T. Hirai, *Org. Biomol. Chem.*, 2010, **8**, 1310–1314.
63 D. Srikun, E. W. Miller, D. W. Dornaille and C. J. Chang, *J. Am. Chem. Soc.*, 2008, **130**, 4596–4597.
64 I. Berndt and W. Richtering, *Macromolecules*, 2003, **36**, 8780–8785.
65 K. Horie, S. Yamada, S. Machida, S. Takahashi, Y. Isono and H. Kawaguchi, *Macromol. Chem. Phys.*, 2003, **204**, 131–138.
66 R. Pelton, *Adv. Colloid Interface Sci.*, 2000, **85**, 1–33.
67 K. Iwai, Y. Matsumura, S. Uchiyama and A. P. de Silva, *J. Mater. Chem.*, 2005, **15**, 2796–2800.
68 S. Uchiyama, N. Kawai, A. P. de Silva and K. Iwai, *J. Am. Chem. Soc.*, 2004, **126**, 3032–3033.
69 S. Uchiyama, Y. Matsumura, A. P. de Silva and K. Iwai, *Anal. Chem.*, 2003, **75**, 5926–5935.
70 M. Q. Zhu, L. Y. Zhu, J. J. Han, W. W. Wu, J. K. Hurst and A. D. Q. Li, *J. Am. Chem. Soc.*, 2006, **128**, 4303–4309.
71 Y. Shiraishi, R. Miyarnoto and T. Hirai, *Langmuir*, 2008, **24**, 4273–4279.
72 C. H. Li, Y. X. Zhang, J. M. Hu, J. J. Cheng and S. Y. Liu, *Angew. Chem., Int. Ed.*, 2010, **49**, 5120–5124.

Published on 23 November 2010 on http://pubs.rsc.org | doi:10.1039/C0JM01828G
Downloaded by University of Science and Technology of China on 30 November 2010